



# Errors in the IMEX-BDF-OS methods for pricing American style options under the jump-diffusion model

Deepak Kumar Yadav<sup>1</sup> · Akanksha Bhardwaj<sup>2</sup> · Alpesh Kumar<sup>1</sup>

Received: 14 November 2022 / Revised: 16 June 2023 / Accepted: 17 October 2023 /  
Published online: 6 December 2023

© The Author(s) under exclusive licence to Sociedade Brasileira de Matemática Aplicada e Computacional 2023

## Abstract

The operator splitting method has been effectively applied to jump-diffusion models, and it is also easy to implement because the differential and complementarity restrictions are decoupled and solved separately. Despite their ubiquity, these operator-splitting approaches for jump-diffusion models have no stability and error analysis. In this direction, we performed a priori stability analysis for the implicit–explicit backward difference operator splitting techniques (IMEX-BDF-OS). After the stability analysis, we established the error estimates for IMEX-BDF1-OS and IMEX-BDF2-OS techniques. To validate the theoretical results, numerical evidence of the pricing of American options under Kou’s and Merton’s jump-diffusion models has been shown.

**Keywords** Operator splitting · Jump-diffusion · American options · Linear complementarity problems · Stability analysis · Error analysis

**Mathematics Subject Classification** 65M06 · 65M12 · 65M15

## 1 Introduction

One of the most extensively used models in option pricing is the Black–Scholes (BS). The stock price in the classical Black–Scholes model is a standard Wiener process that is continu-

---

Communicated by Dan Goreac.

✉ Alpesh Kumar  
alpeshk@rgipt.ac.in; alpeshmath@gmail.com

Deepak Kumar Yadav  
20bs0006@rgipt.ac.in; mathematicsdeepak28@gmail.com

Akanksha Bhardwaj  
akankshabhardwaj@soa.ac.in; bhardwaj.ak11@gmail.com

<sup>1</sup> Department of Mathematical Sciences, Rajiv Gandhi Institute of Petroleum Technology, Jais Amethi 229304, India

<sup>2</sup> Centre for Data Science, Institute of Technical Education and Research (ITER), Siksha ‘O’ Anusandhan (Deemed to be University), Bhubaneswar, Odisha, India

ous in time. Jumps can occur at any time, and the log-normal distribution characteristic of the stock price cannot capture these jumps in the classical Black–Scholes model. Several models have been developed in the literature to overcome the above problem. Merton's (1976) and Kou's (2002) jump-diffusion models are the most frequently applied models among them. For the jump-amplitudes, Merton recommended a log-normally distributed process, whereas Kou proposed a log-double-exponentially distributed process.

To evaluate the price of the American option under the jump-diffusion process, the solution of a linear complementarity problem having a non-local integral operator is required. In order to, many methods have been proposed in the literature to solve the discretized linear complementarity problem arising in American option pricing.

For these types of problems, Kwon and Lee (2011) proposed a three-time levels implicit numerical method combined with an operator splitting technique to approximate the value of American options where the underlying asset acts in accordance with a jump-diffusion model. Huang et al. (2013) proposed the finite difference technique under the jump-diffusion model on a piecewise uniform grid with the help of a penalty approach for pricing the American put options. Huan et al. (2011) analyzed a number of techniques with penalty approach for pricing American options under a regime switching stochastic process. Salmi and Toivanen (2011, 2014) proposed an iterative method and a family of implicit–explicit time discretization techniques for option pricing problems. To handle the different boundary conditions and non-smooth initial conditions for numerous underlying claims, Chen et al. (2012) presented a spectral element method, Pindza et al. (2014) established a robust spectral technique, Company et al. (2021) proposed a front-fixing exponential time differencing (FF-ETD) technique, Kumar and Deswal (2021) provided a wavelet-based approximation approach for examining the sensitivity and value of American options determined by LCPs. Wang et al. (2019) show the stability and error estimations of the variable step-size IMEX BDF2 approach applied to the abstract partial integro-differential equation with nonsmooth initial data, which demonstrates the jump-diffusion option pricing model in finance. They gave the stability analysis and derived the consistency error and the global error bounds for the variable step-size IMEX BDF2 method up to the second order for the European style option and explored the possibilities for the American style option.

In recent works, Kadalbajoo et al. (2015a, b, 2016) examined the efficiency of the meshfree method to deal with option pricing problems based on the local radial basis function for numerically solving the multi-dimensional option pricing problem and solved the PIDE that occurs when the underlying asset act in accordance with the jump-diffusion process using an RBF-based approach. Saib et al. (2012) come up with a differential quadrature rule based on RBF for spatial discretization along with integration with respect to exponential time to work under the jump-diffusion model, Yousuf et al. (2018) solved the complex PIDE systems and Thakoor et al. (2018) devised a compact-RBF scheme with the use of local mesh refinement scheme which helps to achieve the higher order accuracy. Dehghan et al. (2018) presented a new class of radial basis function and explored its efficiency in option pricing problems. Haghi et al. (2018) introduced a new combination of an RBF-based finite difference method, and Bastani et al. (2013) presented an RBF-based collocation method for pricing American options. Some other mesh free works for option pricing problems can be found in Mollapourasl et al. (2018); Rad and Parand (2017) and reference therein.

Further, Akbari et al. (2019) also used a compact finite difference scheme to evaluate the option value under the exponential jump-diffusion models, Patel and Mehra (2018) presented a fourth-order compact method to evaluate the option value under the Kou's and Merton's jump-diffusion models, other authors (Chen et al. 2019; Düring and Pitkin 2019; Thakoor et al. 2013) also used the compact finite difference schemes for option pricing models. To

solve parabolic PIDEs with non-smooth payoff function, Wang et al. (2021) developed an IMEX midpoint formula with variable spatial step sizes and variable time steps. In del Carmen Calvo-Garrido and Vázquez (2015), the authors show the effects of jump-diffusion models for the house price evolution in the pricing of fixed-rate mortgages with prepayment and default options. Tour et al. (2020) introduced a spectral element method to evaluate the price of the option. The mesh-free moving least-squares approximation is used in Shirzadi et al. (2020) to evaluate the price of multi-asset options under the jump-diffusion processes.

To mitigate the iterative procedure, we employed the Backward difference IMEX methodology with the association of the operator splitting approach to evaluate the price of an American option. Operator splitting technique has been used proficiently for several Black–Scholes models (Chen and Shen 2020; Cho et al. 2022; Ikonen and Toivanen 2009; Kazmi 2019; Li et al. 2019; Patel and Mehra 2017; Xu et al. 2022). In recent research, Chen et al. (2019) developed a new OS technique for pricing the value of American options under the time-fractional Black–Scholes models, Boen and In’t Hout (2020) present the operator splitting strategies for two-asset Merton jump-diffusion model. OS techniques are durable to apply since the differential equation and complementarity conditions are disentangled and rapidly solved on their own. But beyond their omnipresence, these operator-splitting approaches still lack some mathematical support. Recently, Chen and Shen (2020) had established the stability results for BDF1 operator splitting (BDF1-OS) and BDF2 operator splitting (BDF2-OS) methods along with error analysis of BDF1-OS method for Black–Scholes model. Throughout this paper, we primarily concentrated on the stability and error analysis of the operator splitting method for the jump-diffusion model and undergo careful investigation of the related numerical techniques. We showed the stability and error estimates for IMEX-BDF1-OS and IMEX-BDF2-OS techniques to solve LCPs arising in the American option pricing under the jump-diffusion model.

The rest of the manuscript is structured in the following manner. We started with introducing the jump-diffusion model, describing the basic notations, symbols, and presumptions used throughout this paper and the construction of the LCP and its associated characteristics. In Sect. 3, we put forward the operator splitting methods, and in Sect. 4, we verify their stability analysis. In Sect. 5, we have shown the error estimates for IMEX-BDF1-OS, IMEX-BDF2-OS methods. In Sect. 6, we put forth some numerical outcomes to verify our theoretical results and associated discussions.

## 2 The Jump–Diffusion model

Consider an asset with price  $S$  and the stochastic differential equation (SDE) that represents the fluctuation of the stock price.

$$\frac{dS}{S} = (\nu - \kappa\lambda)d\tau + \sigma dZ + (\eta - 1)dq, \tag{2.0.1}$$

where  $\tau$  is the time to maturity,  $dZ$  is an enhancement of standard Gauss–Wiener process,  $\nu$  is drift rate,  $\sigma$  is nonzero constant volatility and  $\lambda$  is taken as the intensity of the independent Poisson process  $dq$ , where

$$dq = \begin{cases} 0 & \text{if probability is } 1 - \lambda d\tau, \\ 1 & \text{if probability is } \lambda d\tau. \end{cases}$$

$\kappa$  is expected relative jump size that is  $\kappa = \mathbb{E}(\eta - 1)$ , where  $\mathbb{E}[\cdot]$  represent the expectation operator and  $\eta - 1$  is an impulse function producing jump from  $S$  to  $S_\eta$ . To put it in another

way, the arrival of a jump is stochastic, and this is a feature of the stochastic differential equation for  $S$ . As a result, there are two sources of uncertainty. To begin with, the term  $dZ$  denotes typical Brownian motion, and the term  $dq$  denotes exceptional and infrequent events. Geometric Brownian motion and pure jump-diffusion are two particular examples of Eq. (2.0.1). If the Poisson event does not occur ( $dq = 0$ ), then Eq. (2.0.1) is equivalent to the usual stochastic process of geometric Brownian motion assumed in the Black–Scholes model.

If, on the other hand, the Poisson event occurs, then Eq. (2.0.1) can be written as

$$\frac{dS}{S} \simeq \eta - 1.$$

In this situation, most of the time, the path of  $S$  is continuous, but finite positive or negative jumps may appear at discrete points in time. We assume that the jumps and Brownian motion are independent.

Let  $V(S, \tau)$  represent the value of the American option, which depends on the asset price  $S$  with current time  $\tau$ . As we can exercise the American option at any time up to the life of the option, and we can formulate it as the linear complementarity problem (LCP) based on the stochastic differential Eq. (2.0.1)

$$\begin{cases} \frac{\partial V}{\partial \tau} + \mathcal{L}V \leq 0, & (S, \tau) \in [0, \infty) \times [0, T) \\ V(S, \tau) - \Phi(S) \geq 0, & (S, \tau) \in [0, \infty) \times [0, T) \\ (\frac{\partial V}{\partial \tau} + \mathcal{L}V)(V(S, \tau) - \Phi(S)) = 0 & (S, \tau) \in [0, \infty) \times [0, T) \\ V(S, T) = \Phi(S) & S \in [0, \infty). \end{cases} \quad (2.0.2)$$

The spatial operator  $\mathcal{L}$  can be defined as:

$$\mathcal{L}V(S, \tau) = \frac{1}{2}\sigma^2 S^2 \frac{\partial^2 V}{\partial S^2} + (r - \lambda\kappa)S \frac{\partial V}{\partial S} - (r + \lambda)V + \lambda \int_0^\infty V(S\eta)g(\eta)d\eta, \quad (2.0.3)$$

where  $S$  is the stock price of any asset at time  $\tau$  with constant volatility  $\sigma \neq 0$  and interest rate  $r$ , and the probability density function of the jump with amplitude  $\eta$  is given by  $g(\eta)$ .

Here,  $g(\eta)$  follow the given properties:  $g(\eta) \geq 0, \forall \eta$  and  $\int_0^\infty g(\eta)d\eta = 1$ .

The option value  $V(S, T)$  at the time of maturity  $T$  is termed as pay-off function. For the put option, the pay-off function is given by:

$$\Phi(S) = \max(K - S, 0) \quad (2.0.4)$$

with the strike price  $K$ .

For the Merton’s jump-diffusion model,  $g(\eta)$  represent the log-normal density

$$g(\eta) := \frac{1}{\sqrt{2\pi\sigma_J\eta}} \exp\left[-\frac{(\ln \eta - \mu_J)^2}{2\sigma_J^2}\right],$$

where  $\kappa := \mathbb{E}(\eta - 1) = \exp\left(\mu_J + \frac{\sigma_J^2}{2}\right) - 1$ , and  $\mu_J$  and  $\sigma_J^2$  are the mean and the variance of jump in return, respectively.

Under the Kou’s model  $g(\eta)$  follows the log-double-exponential density

$$g(\eta) := \frac{1}{\eta} \left( p\eta_1 e^{-\eta_1 \ln(\eta)} \mathcal{H}(\ln(\eta)) + q\eta_2 e^{-\eta_2 \ln(\eta)} \mathcal{H}(-\ln(\eta)) \right),$$

where  $\mathcal{H}(\cdot)$  represents a Heaviside function with  $p > 0, q = 1 - p, \eta_1 > 1, \eta_2 > 0$  and  $\kappa$  is given by  $\kappa := \frac{p\eta_1}{\eta_1 - 1} + \frac{q\eta_2}{\eta_1 + 1} - 1$ .

Further, since the problem (2.0.2) is degenerate and backward in time so we can transform it into a non-degenerate and forward in time problem by using the transformations  $x = \ln(\frac{S}{K}), y = \ln(\eta), t = T - \tau$  and  $v(x, t) := V(Ke^x, T - \tau)$ , i.e.

$$\begin{cases} \frac{\partial v}{\partial t} - \mathcal{L}v \geq 0 & (x, t) \in \mathbb{R} \times J, \\ v(x, t) - \Phi(Ke^x) \geq 0 & (x, t) \in \mathbb{R} \times J, \\ (\frac{\partial v}{\partial t} - \mathcal{L}v)(v(x, t) - \Phi(Ke^x)) = 0 & (x, t) \in \mathbb{R} \times J, \\ v(x, 0) = \Phi(Ke^x) & x \in \mathbb{R}, \end{cases} \tag{2.0.5}$$

where  $J = (0, T]$  and the spatial operator can be defined as

$$\mathcal{L}v(x, t) = \frac{1}{2}\sigma^2 \frac{\partial^2 v}{\partial x^2} + \left(r - \frac{\sigma^2}{2} - d - \lambda\kappa\right) \frac{\partial v}{\partial x} - (r + \lambda)v + \lambda \int_{-\infty}^{\infty} v(y, t) f(y - x) dy. \tag{2.0.6}$$

We have,  $\mathcal{L} = \mathcal{D} + \mathcal{I}$ , where  $\mathcal{D}$  represents the differential operator and  $\mathcal{I}$  is used as an integral operator, such that

$$\mathcal{D}v(x, t) = \frac{1}{2}\sigma^2 \frac{\partial^2 v}{\partial x^2} + \left(r - \frac{\sigma^2}{2} - d - \lambda\kappa\right) \frac{\partial v}{\partial x} - (r + \lambda)v, \tag{2.0.7}$$

$$\mathcal{I}v(x, t) = \lambda \int_{-\infty}^{\infty} v(y, t) f(y - x) dy. \tag{2.0.8}$$

After applying the given transformation, we can write the function  $f(y)$  as:

$$f(y) := \begin{cases} \frac{1}{\sqrt{2\pi\sigma_J}} \exp(-\frac{(y-\mu_J)^2}{2\sigma_J^2}) & \text{Merton's model,} \\ p\eta_1 e^{-\eta_1 y} \mathcal{H}(y) + q\eta_2 e^{-\eta_2 y} \mathcal{H}(-y) & \text{Kou's model.} \end{cases}$$

To approximate the integral term on truncated domain  $\Omega$ , we used the composite trapezoidal rule.

For evaluational purposes, we localized the problem (2.0.5) on a bounded domain  $\Omega := (x^L, x^R)$  with  $x^L$  and  $x^R \in \mathbb{R}$ . Now, considering  $u(x, t)$  as a solution of the following localized problem (2.0.9)

$$\begin{cases} \frac{\partial u}{\partial t} - \mathcal{L}u \geq 0 & (x, t) \in \Omega \times J, \\ u(x, t) - \Phi(Ke^x) \geq 0 & (x, t) \in \Omega \times J, \\ (\frac{\partial u}{\partial t} - \mathcal{L}u)(u(x, t) - \Phi(Ke^x)) = 0 & (x, t) \in \Omega \times J, \\ u(x, 0) = \Phi(Ke^x) & x \in \Omega, \end{cases} \tag{2.0.9}$$

with

$$u(x, t) = B(x, t), \quad (x, t) \in \Omega^c \times \bar{J},$$

and

$$B(x, t) = \begin{cases} \Phi(Ke^x) : & (x, t) \in \partial\Omega \times \bar{J}, \\ \Phi(Ke^x) : & (x, t) \in (\bar{\Omega}^c \cap \bar{\Omega}_{Big}) \times \bar{J}, \Omega \subseteq \Omega_{Big}, \\ 0 & : & (x, t) \in \bar{\Omega}_{Big}^c \times \bar{J}. \end{cases}$$

Here,  $\partial\Omega$  represents the boundary of  $\Omega$ ,  $\Omega^c = \mathbb{R} \setminus \Omega$ ,  $\bar{J} = [0, T]$  and  $\Omega_{Big}$  is an open connected and bounded subset of  $\mathbb{R}$  (See, for example, Kadalbajoo et al. (2015b)).

The problems (2.0.2) and (2.0.9) are stated to have unique solutions under specific assumptions relating to the coefficients of the spatial operator  $\mathcal{L}$ . Moreover, within the interior of the domain, the localization error due to the domain truncation decreases exponentially with respect to the domain size (see, for example, Cont and Voltchkova 2005; Garroni et al. 1992; Matache et al. 2004).

### 3 Operator splitting methods

Ikonen and Toivanen (2004) introduced the operator splitting approach for pricing the value of the American put option. The primary idea behind introducing the operator splitting technique is to derive an expression with the help of an additional variable  $\psi$  such that  $\psi = u_t - \mathcal{L}u$ .

We can reformulate LCP (2.0.9) as

$$\begin{cases} \frac{\partial u}{\partial t} - \mathcal{L}u = \psi, \\ u(x, t) - \Phi(K e^x) \cdot \psi = 0, \\ u(x, t) - \Phi(K e^x) \geq 0, \\ \psi \geq 0, \end{cases} \tag{3.0.1}$$

in the region  $\Omega \times J$ .

Let the system (3.0.1) be initially discretized in time with uniform grid  $t_n = nk$ ,  $n = 0, 1, 2, \dots, N$  with temporal mesh length  $k$  and  $N + 1$  to be the total numbers of temporal mesh points. Where  $u(x, t_n)$  abbreviated as  $u_n$ .

Now, we briefly discussed the IMEX-BDF-OS methods for the temporal discretization of LCP (3.0.1).

#### 3.1 IMEX-BDF1-OS method

Let us split the governing equation  $u_t - \mathcal{L}u = \psi$  into two discrete equations on the  $(n + 1)$ th time level as

$$\left( \frac{\tilde{u}_{n+1} - u_n}{k} \right) - \mathcal{D}\tilde{u}_{n+1} - \lambda\mathcal{I}(u_n) = \psi_n, \tag{3.1.1}$$

$$\left( \frac{u_{n+1} - u_n}{k} \right) - \mathcal{D}\tilde{u}_{n+1} - \lambda\mathcal{I}(u_n) = \psi_{n+1}. \tag{3.1.2}$$

Here, the discrete problem for LCP (3.0.1) is to find the pair  $(u_{n+1}, \psi_{n+1})$  that satisfy the discrete equations (3.1.1) and (3.1.2) as well as the constraints,

$$\begin{cases} u_{n+1} \geq \Phi, \\ \psi_{n+1} \geq 0, \\ \psi_{n+1}(u_{n+1} - \Phi) = 0. \end{cases} \tag{3.1.3}$$

We will compute the solution of (3.0.1) using the IMEX-BDF1-OS techniques in two steps. First, we determine the intermediate approximation  $\tilde{u}_{n+1}$  with the help of Eq. (3.1.1) under given boundary conditions

$$\tilde{u}_{n+1}(x^L) = K, \quad \tilde{u}_{n+1}(x^R) = 0,$$

and the known auxiliary term  $\psi_n$ .

Second, we develop a relationship between  $u_{n+1}$  and  $\psi_{n+1}$  in (3.1.2). To do so, we restate the Eq. (3.1.2) as a problem, combining Eq. (3.1.1) and the restrictions in (3.1.3) in order to determine the pair  $(u_{n+1}, \psi_{n+1})$ , such that

$$\begin{cases} \frac{u_{n+1} - \tilde{u}_{n+1}}{k} = \psi_{n+1} - \psi_n, \\ \psi_{n+1}(u_{n+1} - \Phi) = 0, \end{cases} \tag{3.1.4}$$

with the constraints

$$u_{n+1} \geq \Phi \text{ and } \psi_{n+1} \geq 0. \tag{3.1.5}$$

Again, by solving the problems (3.1.4)–(3.1.5) in  $(u_{n+1}, \psi_{n+1})$  plane, we get

$$(u_{n+1}, \psi_{n+1}) = \begin{cases} (\Phi, \psi_n + \frac{\Phi - \tilde{u}_{n+1}}{k}) & \text{if } \tilde{u}_{n+1} - k\psi_n \leq \Phi, \\ (\tilde{u}_{n+1} - k\psi_n, 0) & \text{otherwise.} \end{cases} \tag{3.1.6}$$

As a result, the second step may be completed by solving the discrete equation (3.1.1) using the modified formula (3.1.6). Using initial condition and assigning value  $\psi_0 = 0$  on the zeroth time level, the pair  $(u_0, \psi_0)$  may be achieved. One can use the algorithm discussed in Kwon and Lee (2011).

### 3.2 IMEX-BDF2-OS method

Let us assume that the values  $\{u_n, \psi_n\}$  and  $\{u_{n-1}, \psi_{n-1}\}$  are a priori, known at the points  $t_n$  and  $t_{n-1}$ . We perform two sub-steps at discrete point  $t_{n+1}$ . In first step, we compute an intermediate value  $\tilde{u}_{n+1}$  using the following BVP (3.2.1)

$$\begin{cases} \frac{1}{k} \left( \frac{3}{2}\tilde{u}_{n+1} - 2u_n + \frac{1}{2}u_{n-1} \right) - \mathcal{D}\tilde{u}_{n+1} - \lambda \mathcal{I}(\mathcal{E}u_n) = \psi_n, \\ \tilde{u}_{n+1}(x^L) = K, \quad \tilde{u}_{n+1}(x^R) = 0, \end{cases} \tag{3.2.1}$$

where  $\mathcal{E}u_n = 2u_n - u_{n-1}$ .

In the second step of the operator splitting method, we project the  $\tilde{u}_{n+1}$  on constraint space to obtain  $u_{n+1}$  with the following correction terms

$$\begin{cases} \frac{3(u_{n+1} - \tilde{u}_{n+1})}{2k} = \psi_{n+1} - \psi_n, \\ u_{n+1} \geq \Phi, \\ \psi_{n+1} \geq 0, \\ \psi_{n+1}(u_{n+1} - \Phi) = 0. \end{cases} \tag{3.2.2}$$

Now, by solving the problems (3.2.1)–(3.2.2) in  $(u_{n+1}, \psi_{n+1})$  plane, we get

$$(u_{n+1}, \psi_{n+1}) = \begin{cases} (\Phi, \psi_n + \frac{3}{2} \frac{\Phi - \tilde{u}_{n+1}}{k}) & \text{if } \tilde{u}_{n+1} - \frac{2k}{3}\psi_n \leq \Phi, \\ (\tilde{u}_{n+1} - \frac{2k}{3}\psi_n, 0) & \text{otherwise.} \end{cases} \tag{3.2.3}$$

Thus, the first step may be accomplished by solving a discrete Eq. (3.2.1), and the second step can be performed by using the updating formula (3.2.3). The value on the previous two-time levels is required by the implicit technique with three-time levels, as described above. Using starting condition and assigning value  $\psi_0 = 0$ , the pair  $(u_0, \psi_0)$  on the zeroth time level may be achieved. Alternatively, one can also use the algorithm discussed in Kwon and Lee (2011). We shall use the IMEX-BDF1-OS method to find the pair  $(u_1, \psi_1)$  at first level.

### 4 Stability analysis

For theoretical convenience, let us transform the problem (3.0.1) into a problem with homogeneous boundary conditions without loss of generality, i.e.,

$$\begin{cases} \frac{\partial w}{\partial t} - \mathcal{L}w = \psi + f, & (x, t) \in \Omega \times J, \\ (w(x, t) - w_0(x)) \cdot \psi = 0, & (x, t) \in \Omega \times J, \\ w(x, t) - w_0(x) \geq 0, & (x, t) \in \Omega \times J, \\ \psi \geq 0, & (x, t) \in \Omega \times J, \\ w(x, 0) = w_0(x), & x \in \Omega \\ w(x, t) = 0, & (x, t) \in \partial\Omega \times \bar{J}, \end{cases} \tag{4.0.1}$$

where  $w_0(x) := \Phi(Ke^x) - \phi(x)$ ,  $w(x, t) = u(x, t) - \phi(x)$  and  $f = \mathcal{L}\phi$ ,  $x \in \mathbb{R}$ , and

$$\phi(x) = \begin{cases} \frac{x^R - x}{x^R - x^L} \Phi(Ke^{x^L}) + \frac{x - x^L}{x^R - x^L} \Phi(Ke^{x^R}) : x \in \bar{\Omega}, \\ \Phi(Ke^x) : x \in \bar{\Omega}^C \cap \bar{\Omega}_{Big}, \\ 0 : x \in \bar{\Omega}_{Big}^C. \end{cases}$$

Alternatively, one can also find this algorithm in Kadalbajoo et al. (2015b).

**Lemma 1** (Discrete Gronwall’s Lemma) *Suppose that  $\alpha_n$  is a non-negative sequence, and that the sequence  $\beta_n$  satisfies*

$$\begin{cases} \beta_0 \leq \delta_0, \\ \beta_n \leq \delta_0 + \sum_{k=0}^{n-1} \gamma_k + \sum_{k=0}^{n-1} \alpha_k \beta_k \quad n \geq 1, \end{cases}$$

then  $\beta_n$  satisfies

$$\begin{cases} \beta_1 \leq \delta_0(1 + \alpha_0) + \gamma_0, \\ \beta_n \leq \delta_0 \prod_{k=0}^{n-1} (1 + \alpha_k) + \sum_{k=0}^{n-2} \gamma_k \prod_{s=k+1}^{n-1} (1 + \alpha_s) + \gamma_{n-1} \quad n \geq 2. \end{cases}$$

Moreover, if  $\delta_0 \geq 0$  and  $\gamma_n \geq 0$  for  $n \geq 0$ , it follows

$$\beta_n \leq \left( \delta_0 + \sum_{k=0}^{n-1} \gamma_k \right) \exp\left( \sum_{k=0}^{n-1} \alpha_k \right), \quad n \geq 1.$$

**Proof** See Quarteroni and Valli (2008). □

#### 4.1 Identities and inequalities

We will frequently use the following identities and inequalities in the stability and error analysis.

$$(Dw, w) \leq \alpha \|w\|^2, \tag{I1}$$

$$(a, b) \leq \epsilon a^2 + \frac{1}{4\epsilon} b^2, \quad a, b \in \mathbb{R} \text{ and } \epsilon > 0, \tag{I2}$$

$$2(a - b, a) = \|a\|^2 - \|b\|^2 + \|a - b\|^2, \tag{I3}$$



$$2(3a - 4b + c, a) = a^2 + (2a - b)^2 - b^2 - (2b - c)^2 + (a - 2b + c)^2, \tag{I4}$$

where  $\alpha = \left| \frac{(r - \frac{\sigma^2}{2} - \lambda\kappa)^2 - (2(r + \lambda)\sigma^2)}{2\sigma^2} \right|$ , and for the proof of inequality (I1), one can see Kadalbajoo et al. (2016) and reference therein.

We shall use the following result in the analysis, for all  $w(\cdot, t) \in L^2(\Omega)$ ,  $t \in (0, T)$  such that

$$\bar{w}(x, t) = \begin{cases} w(x, t) & : (x, t) \in \Omega \times [0, T], \\ 0 & : (x, t) \in \Omega^c \times [0, T]. \end{cases}$$

The integral operator  $\mathcal{I}(w)$  follow the condition  $\|\mathcal{I}\bar{w}(\cdot, t)\| \leq C_I \|w(\cdot, t)\|$ , where  $C_I$  is a constant that is independent to  $t$  and  $\|u\| := (\int_{\Omega} |u(x)|^2 dx)^{\frac{1}{2}}$ .

### 4.2 Stability analysis for IMEX-BDF1-OS

**Theorem 1** Under the assumption  $k < \frac{1}{2(4\alpha + 1 + \lambda C_I)}$ , the scheme is stable,  $\forall 1 \leq m \leq \frac{T}{k}$  in the following sense:

$$\begin{aligned} \|w_m\|^2 + \frac{1}{2} \sum_{n=0}^{m-1} \|\tilde{w}_{n+1} - w_n\|^2 + k^2 \|\psi_m\|^2 \leq C & \left( \|w_0\|^2 + k \|\psi_0\|^2 + k \sum_{n=0}^{m-1} \|w_0\|^2 \right. \\ & \left. + k \sum_{n=0}^{m-1} \|f\|^2 + k \sum_{n=0}^{m-1} \|\psi_n\|^2 \right), \end{aligned}$$

where  $C$  is a constant that depends on the parameters  $C_I, r, \sigma, \lambda$  and  $T$ , but may not be the same at each occurrence.

**Proof** Consider the Eq. (4.0.1)

$$\frac{\tilde{w}_{n+1} - w_n}{k} = \mathcal{D}\tilde{w}_{n+1} + \lambda\mathcal{I}(w_n) + f + \psi_n. \tag{4.2.1}$$

After taking the inner product of both sides of (4.2.1) with  $4k\tilde{w}_{n+1}$  and using the identities (I3) and (I1), we have

$$\begin{aligned} 2\|\tilde{w}_{n+1}\|^2 - 2\|w_n\|^2 + 2\|\tilde{w}_{n+1} - w_n\|^2 \\ \leq 4k\alpha \|\tilde{w}_{n+1}\|^2 + 4k\lambda(\mathcal{I}(w_n), \tilde{w}_{n+1}) + 4k(f, \tilde{w}_{n+1}) + 4k(\psi_n, \tilde{w}_{n+1}). \end{aligned} \tag{4.2.2}$$

Consider the Eq. (3.1.4), we have

$$w_{n+1} - w_0 - k\psi_{n+1} = \tilde{w}_{n+1} - w_0 - k\psi_n. \tag{4.2.3}$$

Taking the inner product of both sides of (4.2.3) with itself and using some inequalities from Sect. 4.1, we have

$$\begin{aligned} \|w_{n+1}\|^2 + \|w_0\|^2 - \frac{1}{2} \|w_{n+1}\|^2 - 2\|w_0\|^2 + k^2 \|\psi_{n+1}\|^2 - 2k(w_{n+1} - w_0, \psi_{n+1}) \\ \leq 2\|\tilde{w}_{n+1}\|^2 + 2\|w_0\|^2 + k^2 \|\psi_n\|^2 - 2k(\tilde{w}_{n+1}, \psi_n) + 2k(w_0, \psi_n). \end{aligned} \tag{4.2.4}$$

Now, adding up the inequalities (4.2.2) and (4.2.4) with the use of  $(w_{n+1} - w_0, \psi_{n+1}) = 0$ , we get

$$\begin{aligned} & \frac{1}{2} \|w_{n+1}\|^2 - 2\|w_n\|^2 + 2\|\tilde{w}_{n+1} - w_n\|^2 + k^2(\|\psi_{n+1}\|^2 - \|\psi_n\|^2) \\ & \leq 3\|w_0\|^2 + 4k\alpha\|\tilde{w}_{n+1}\|^2 + 4k\lambda(\mathcal{I}(w_n), \tilde{w}_{n+1}) + 4k(f, \tilde{w}_{n+1}) \\ & \quad + 2k(\tilde{w}_{n+1}, \psi_n) + 2k(w_0, \psi_n). \end{aligned}$$

After small calculations

$$\begin{aligned} & \frac{1}{2} \|w_{n+1}\|^2 - \frac{1}{2} \|w_n\|^2 + \frac{3}{2} \|\tilde{w}_{n+1} - w_n\|^2 + k^2(\|\psi_{n+1}\|^2 - \|\psi_n\|^2) \\ & \leq 3\|w_0\|^2 + 2k(4\alpha + 1 + \lambda C_I)\|\tilde{w}_{n+1} - w_n\|^2 \\ & \quad + \left(2k(4\alpha + 1 + \lambda C_I) + 4k\lambda C_I + \frac{3}{2}\right)\|w_n\|^2 \\ & \quad + 8k\|f\|^2 + 2k\|\psi_n\|^2 + k\|w_0\|^2 + k\|\psi_n\|^2. \end{aligned}$$

Assuming that  $k < \frac{1}{2(4\alpha+1+\lambda C_I)}$ , we get

$$\begin{aligned} & \frac{1}{2} \|w_{n+1}\|^2 - \frac{1}{2} \|w_n\|^2 + \frac{1}{2} \|\tilde{w}_{n+1} - w_n\|^2 + k^2(\|\psi_{n+1}\|^2 - \|\psi_n\|^2) \\ & \leq 3\|w_0\|^2 + \left(2k(4\alpha + 1 + \lambda C_I) + 4k\lambda C_I + \frac{3}{2}\right)\|w_n\|^2 \\ & \quad + 8k\|f\|^2 + 2k\|\psi_n\|^2 + k\|w_0\|^2 + k\|\psi_n\|^2. \end{aligned}$$

Taking the summation on both sides of the above inequality from  $n = 0$  to  $m - 1$

$$\begin{aligned} & \|w_m\|^2 + \sum_{n=0}^{m-1} \|\tilde{w}_{n+1} - w_n\|^2 + 2k^2\|\psi_m\|^2 \\ & \leq \|w_0\|^2 + 2k^2\|\psi_0\|^2 + (6 + 2k) \sum_{n=0}^{m-1} \|w_0\|^2 + (4k(4\alpha + 1 + \lambda C_I) + 8k\lambda C_I + 3) \\ & \quad \sum_{n=0}^{m-1} \|w_n\|^2 + 16k \sum_{n=0}^{m-1} \|f\|^2 + 6k \sum_{n=0}^{m-1} \|\psi_n\|^2. \end{aligned}$$

Applying the Lemma 1, we get,

$$\begin{aligned} & \|w_m\|^2 + \sum_{n=0}^{m-1} \|\tilde{w}_{n+1} - w_n\|^2 + 2k^2\|\psi_m\|^2 \\ & \leq C' \left( \|w_0\|^2 + 2k^2\|\psi_0\|^2 + (6 + 2k) \sum_{n=0}^{m-1} \|w_0\|^2 + 16k \sum_{n=0}^{m-1} \|f\|^2 + 6k \sum_{n=0}^{m-1} \|\psi_n\|^2 \right). \end{aligned} \tag{4.2.5}$$

Further simplifying the inequality (4.2.5), we obtain the desired result,

$$\|w_m\|^2 + \frac{1}{2} \sum_{n=0}^{m-1} \|\tilde{w}_{n+1} - w_n\|^2 + k^2 \|\psi_m\|^2 \leq C \left( \|w_0\|^2 + k \|\psi_0\|^2 + k \sum_{n=0}^{m-1} \|w_0\|^2 + k \sum_{n=0}^{m-1} \|f\|^2 + k \sum_{n=0}^{m-1} \|\psi_n\|^2 \right),$$

where  $C'$  is a constant that depends on the parameters  $C_I, r, \sigma, \lambda$  and  $T$ . □

### 4.3 Stability analysis for IMEX-BDF2-OS

**Theorem 2** Under the assumption  $k < \frac{1}{2(4\alpha+1+\lambda C_I)}$  the scheme is stable,  $\forall 2 \leq m \leq \frac{T}{k}$  in the following sense:

$$\|w_m\|^2 + \|w_{m-1}\|^2 + \frac{1}{2} \sum_{n=1}^{m-1} \|\tilde{w}_{n+1}\|^2 + \frac{8}{9} k^2 \|\psi_m\|^2 \leq C \left( \|w_0\|^2 + \|w_1\|^2 + k \sum_{n=1}^{m-1} \|f\|^2 + k \sum_{n=1}^{m-1} \|w_0\|^2 + k \sum_{n=1}^{m-1} \|\psi_n\|^2 + k^2 \|\psi_1\|^2 \right),$$

where  $C$  is a constant that depends on the parameters  $C_I, r, \sigma, \lambda$  and  $T$ .

**Proof** Consider the Eq. (3.2.1),

$$\frac{3\tilde{w}_{n+1} - 4w_n + w_{n-1}}{2k} = \mathcal{D}\tilde{w}_{n+1} + \lambda \mathcal{I}(\mathcal{E}w_n) + f + \psi_n. \tag{4.3.1}$$

Taking the inner product of both sides of the Eq. (4.3.1) with  $4k\tilde{w}_{n+1}$  and using the identity (I1) and (I4), we have

$$\begin{aligned} & \|\tilde{w}_{n+1}\|^2 - \|w_n\|^2 + \|2\tilde{w}_{n+1} - w_n\|^2 - \|2w_n - w_{n-1}\|^2 + \|\tilde{w}_{n+1} - 2w_n + w_{n-1}\|^2 \\ &= 4k(\mathcal{D}\tilde{w}_{n+1}, \tilde{w}_{n+1}) + 4k\lambda(\mathcal{I}(\mathcal{E}w_n), \tilde{w}_{n+1}) + 4k(f, \tilde{w}_{n+1}) + 4k(\psi_n, \tilde{w}_{n+1}), \\ &\leq 4k\alpha \|\tilde{w}_{n+1}\|^2 + 4k\lambda(\mathcal{I}(\mathcal{E}w_n), \tilde{w}_{n+1}) + 4k(f, \tilde{w}_{n+1}) + 4k(\psi_n, \tilde{w}_{n+1}). \end{aligned} \tag{4.3.2}$$

Now, consider the Eq. (3.2.2)

$$w_{n+1} - w_0 - \frac{2}{3}k\psi_{n+1} = \tilde{w}_{n+1} - w_0 - \frac{2}{3}k\psi_n. \tag{4.3.3}$$

Taking inner product of (4.3.3) from both sides with itself, we have

$$\begin{aligned} & \|w_{n+1} - w_0\|^2 + \frac{4}{9}k^2 \|\psi_{n+1}\|^2 - \frac{4}{3}k(w_{n+1} - w_0, \psi_{n+1}) = \|\tilde{w}_{n+1} - w_0\|^2 + \frac{4}{9}k^2 \|\psi_n\|^2 \\ & - \frac{4}{3}k(\tilde{w}_{n+1} - w_0, \psi_n). \end{aligned}$$

Using some inequalities from Sect. 4.1 and some calculations, we have

$$\begin{aligned} & \|w_{n+1}\|^2 + \|w_0\|^2 - \frac{1}{2}\|w_{n+1}\|^2 - 2\|w_0\|^2 + \frac{4}{9}k^2 \|\psi_{n+1}\|^2 - \frac{4}{3}k(w_{n+1} - w_0, \psi_{n+1}) \\ & \leq 2\|\tilde{w}_{n+1}\|^2 + 2\|w_0\|^2 + \frac{4}{9}k^2 \|\psi_n\|^2 - \frac{4}{3}k(\tilde{w}_{n+1}, \psi_n) + \frac{4}{3}k(w_0, \psi_n). \end{aligned} \tag{4.3.4}$$

Now, multiplying the inequality (4.3.2) by 2 and adding with inequality (4.3.4) and using  $(w_{n+1} - w_0, \psi_{n+1}) = 0$ , we get

$$\begin{aligned} & \frac{1}{2} \|w_{n+1}\|^2 - 2\|w_n\|^2 + 2\|2\tilde{w}_{n+1} - w_n\|^2 - 2\|2w_n - w_{n-1}\|^2 + 2\|\tilde{w}_{n+1} - 2w_n + w_{n-1}\|^2 \\ & \quad + \frac{4}{9}k^2\|\psi_{n+1}\|^2 \\ & \leq 8k\alpha\|\tilde{w}_{n+1}\|^2 + 8k\lambda(\mathcal{I}(\mathcal{E}w_n), \tilde{w}_{n+1}) + 8k(f, \tilde{w}_{n+1}) + 3\|w_0\|^2 + \frac{4}{9}k^2\|\psi_n\|^2 \\ & \quad + \frac{20}{3}k(\tilde{w}_{n+1}, \psi_n) + \frac{4}{3}k(w_0, \psi_n). \end{aligned}$$

After some calculation with the help of some inequalities from Sect. 4.1, we have

$$\begin{aligned} & \|w_{n+1}\|^2 - \|w_n\|^2 + 3\|\tilde{w}_{n+1}\|^2 + 8(\|w_n\|^2 - \|w_{n-1}\|^2) + \frac{8}{9}k^2(\|\psi_{n+1}\|^2 - \|\psi_n\|^2) \\ & \leq \frac{571}{13}\|w_n\|^2 + 32k\lambda C_I\|w_n\|^2 + 8k\lambda C_I\|w_{n-1}\|^2 + 4k(4\alpha + 1 + \lambda C_I)\|\tilde{w}_{n+1}\|^2 \\ & \quad + 32k\|f\|^2 + \frac{212}{9}k\|\psi_n\|^2 + \frac{(4k + 18)}{3}\|w_0\|^2. \end{aligned} \tag{4.3.5}$$

Assuming that  $k < \frac{1}{2(4\alpha+1+\lambda C_I)}$ , then from (4.3.5) we have

$$\begin{aligned} & \|w_{n+1}\|^2 - \|w_n\|^2 + \|\tilde{w}_{n+1}\|^2 + 8(\|w_n\|^2 - \|w_{n-1}\|^2) + \frac{8}{9}k^2(\|\psi_{n+1}\|^2 - \|\psi_n\|^2) \\ & \leq \frac{571}{13}\|w_n\|^2 + 32k\lambda C_I\|w_n\|^2 + 8k\lambda C_I\|w_{n-1}\|^2 + 32k\|f\|^2 \\ & \quad + \frac{212}{9}k\|\psi_n\|^2 + \frac{(4k + 18)}{3}\|w_0\|^2. \end{aligned} \tag{4.3.6}$$

Adding the Eq. (4.3.6) from  $n = 1$  to  $m - 1$

$$\begin{aligned} & \|w_m\|^2 - \|w_1\|^2 + \sum_{n=1}^{m-1} \|\tilde{w}_{n+1}\|^2 + 8\|w_{m-1}\|^2 - 8\|w_0\|^2 + \frac{8}{9}k^2\|\psi_m\|^2 - \frac{8}{9}k^2\|\psi_1\|^2 \\ & \leq \left(\frac{571}{13} + 32k\lambda C_I\right) \sum_{n=1}^{m-1} \|w_n\|^2 + 8k\lambda C_I \sum_{n=1}^{m-1} \|w_{n-1}\|^2 + 32k \sum_{n=1}^{m-1} \|f\|^2 \\ & \quad + \left(\frac{4k + 18}{3}\right) \sum_{n=1}^{m-1} \|w_0\|^2 + \frac{212}{9}k \sum_{n=1}^{m-1} \|\psi_n\|^2. \end{aligned} \tag{4.3.7}$$

$$\begin{aligned} & \|w_m\|^2 + \sum_{n=1}^{m-1} \|\tilde{w}_{n+1}\|^2 + 8\|w_{m-1}\|^2 + \frac{8}{9}k^2\|\psi_m\|^2 \\ & \leq 8\|w_0\|^2 + \|w_1\|^2 + \frac{8}{9}k^2\|\psi_1\|^2 + \left(\frac{571}{13} + 40k\lambda C_I\right) \sum_{n=0}^{m-1} \|w_n\|^2 \\ & \quad + 32k \sum_{n=1}^{m-1} \|f\|^2 + \left(\frac{4k + 18}{3}\right) \sum_{n=1}^{m-1} \|w_0\|^2 + \frac{212k}{9} \sum_{n=1}^{m-1} \|\psi_n\|^2. \end{aligned} \tag{4.3.8}$$

Applying the Lemma 1 on (4.3.8), we have

$$\begin{aligned} & \|w_m\|^2 + \|w_{m-1}\|^2 + \frac{1}{2} \sum_{n=1}^{m-1} \|\tilde{w}_{n+1}\|^2 + \frac{8}{9}k^2\|\psi_m\|^2 \\ & \leq C \left( \|w_0\|^2 + \|w_1\|^2 + k \sum_{n=1}^{m-1} \|f\|^2 + k \sum_{n=1}^{m-1} \|w_0\|^2 + k \sum_{n=1}^{m-1} \|\psi_n\|^2 + k^2\|\psi_1\|^2 \right). \end{aligned} \tag{4.3.9}$$

□

### 5 Error analysis

In the last section, we have established the stability results. Now, we shall derive the corresponding error estimates for IMEX-BDF1-OS and IMEX-BDF2-OS techniques by assuming the exact solution is adequately regular. First, we established the error function and error equation. Denoting the analytic solution at  $t_n$  by  $w(\cdot, t_n)$  and similar for other related variables.

#### 5.1 Error analysis for IMEX-BDF1-OS

We define  $e_n = w(\cdot, t_n) - w_n$ ,  $\tilde{e}_n = w(\cdot, t_n) - \tilde{w}_n$ ,  $h_n = \psi(\cdot, t_n) - \psi_n$  and  $\psi(\cdot, t_{n+1}) - \psi(\cdot, t_n) \leq ck$ , where  $c$  is a generic constant and independent of  $n$ .

From the continuous system (4.0.1), we have

$$\frac{w(\cdot, t_{n+1}) - w(\cdot, t_n)}{k} = \mathcal{D}w(\cdot, t_{n+1}) + \lambda\mathcal{I}(w(t_n)) + f + \psi(\cdot, t_{n+1}) + R_{n+1}, \tag{5.1.1}$$

where  $R_{n+1}$  is truncation error for given method.

Now, we consider the equation for IMEX-BDF1-OS,

$$\frac{\tilde{w}_{n+1} - w_n}{k} = \mathcal{D}(\tilde{w}_{n+1}) + \lambda\mathcal{I}(w_n) + \psi_n + f. \tag{5.1.2}$$

To get the error equation, we subtract (5.1.2) from (5.1.1) and get

$$\frac{\tilde{e}_{n+1} - e_n}{k} = \mathcal{D}(\tilde{e}_{n+1}) + \lambda\mathcal{I}(e_n) + g_n + R_{n+1}, \tag{5.1.3}$$

where  $g_n = \psi(\cdot, t_{n+1}) - \psi_n$ , we can obtain another error equation from (3.1.4), as follows,

$$\frac{e_{n+1} - \tilde{e}_{n+1}}{k} = h_{n+1} - g_n + \psi(t_{n+1}) - \psi(t_n), \tag{5.1.4}$$

or

$$\frac{e_{n+1} - \tilde{e}_{n+1}}{k} = h_{n+1} - g_n, \tag{5.1.5}$$

where  $g_n = h_n + \psi(\cdot, t_{n+1}) - \psi(\cdot, t_n)$  and let  $\psi$  is adequately smooth such that  $\|g_n\| \leq \|h_n\| + ck$ .

**Theorem 3** Under the assumption  $k < \frac{1}{2(4\alpha+1+\lambda C_I)}$ , we have following error estimates for the given method:

$$\|e_m\|^2 + \frac{1}{2} \sum_{n=0}^{m-1} \|\tilde{e}_{n+1}\|^2 \leq Ck^2, \quad \forall 1 \leq m \leq \frac{T}{k}$$

where  $C$  is a constant that depends on the parameters  $C_I, r, \sigma, \lambda$  and  $T$ .

**Proof** Consider the Eq. (5.1.3)

$$\frac{\tilde{e}_{n+1} - e_n}{k} = \mathcal{D}(\tilde{e}_{n+1}) + \lambda \mathcal{I}(e_n) + g_n + R_{n+1}. \tag{5.1.6}$$

Taking the inner product from both sides of (5.1.6) with  $2k(\tilde{e}_{n+1})$  and using the identities (I1) and (I3), we have

$$\begin{aligned} \|\tilde{e}_{n+1}\|^2 - \|e_n\|^2 + \|\tilde{e}_{n+1} - e_n\|^2 &\leq 2k\alpha\|\tilde{e}_{n+1}\|^2 + 2k\lambda C_I \|e_n\| \|\tilde{e}_{n+1}\| \\ &\quad + 2k(g_n, \tilde{e}_{n+1}) + 2k(R_{n+1}, \tilde{e}_{n+1}). \end{aligned} \tag{5.1.7}$$

Consider the Eq. (5.1.5)

$$e_{n+1} - kh_{n+1} = \tilde{e}_{n+1} - kg_n. \tag{5.1.8}$$

Taking inner product of (5.1.8) from both sides, with itself :

$$\|e_{n+1}\|^2 + k^2\|h_{n+1}\|^2 - 2k(e_{n+1}, h_{n+1}) = \|\tilde{e}_{n+1}\|^2 + k^2\|f_n\|^2 - 2k(\tilde{e}_{n+1}, g_n). \tag{5.1.9}$$

Now, adding up the Eqs. (5.1.7) and (5.1.9), and observing that  $2k(e_{n+1}, h_{n+1}) \leq 0$  with the use of some inequalities from Sect. 4.1, we have

$$\begin{aligned} \|e_{n+1}\|^2 - \|e_n\|^2 + \|\tilde{e}_{n+1} - e_n\|^2 + k^2(\|h_{n+1}\|^2 - \|g_n\|^2) \\ \leq k(4\alpha + 1 + \lambda C_I)\|\tilde{e}_{n+1} - e_n\|^2 + k(4\alpha + 3\lambda C_I + 1)\|e_n\|^2 + 4k\|R_{n+1}\|^2 \end{aligned} \tag{5.1.10}$$

Assuming that  $k < \frac{1}{2(4\alpha+1+\lambda C_I)}$ , we have from (5.1.10)

$$\begin{aligned} \|e_{n+1}\|^2 - \|e_n\|^2 + \frac{1}{2}\|\tilde{e}_{n+1} - e_n\|^2 + k^2(\|h_{n+1}\|^2 - \|g_n\|^2) &\leq k(4\alpha + 3\lambda C_I + 1)\|e_n\|^2 \\ &\quad + 4k\|R_{n+1}\|^2. \end{aligned}$$

Adding the above equation from  $n = 0$  to  $m - 1$  and using the result  $\|g_n\|^2 \leq 2\|h_n\|^2 + 2ck^2$  with some calculations, we have

$$\begin{aligned} \|e_m\|^2 - \|e_0\|^2 + \frac{1}{2} \sum_{n=0}^{m-1} \|\tilde{e}_{n+1} - e_n\|^2 + k^2(\|h_m\|^2 - \|h_0\|^2) \\ \leq k(4\alpha + 3\lambda C_I + 1) \sum_{n=0}^{m-1} \|e_n\|^2 + k^2 \sum_{n=0}^{m-1} (\|h_n\|^2 + ck^2) + k \sum_{n=0}^{m-1} \|R_{n+1}\|^2. \end{aligned}$$

Applying the Lemma 1, we get the desired result

$$\|e_m\|^2 + \frac{1}{2} \sum_{n=0}^{m-1} \|\tilde{e}_{n+1} - e_n\|^2 \leq Ck^2.$$

□

### 5.2 Error analysis for IMEX-BDF2-OS

Similarly, for IMEX-BDF2-OS, the error equations are as follows;

$$\frac{3\tilde{e}_{n+1} - 4e_n + e_{n-1}}{2k} = \mathcal{D}(\tilde{e}_{n+1}) + \lambda\mathcal{I}(\mathcal{E}e_n) + g_n + R_{n+1}, \tag{5.2.1}$$

and

$$\frac{3(e_{n+1} - \tilde{e}_{n+1})}{2k} = h_{n+1} - g_n. \tag{5.2.2}$$

**Theorem 4** Under the assumption  $k < \frac{1}{2(4\alpha+1+\lambda C_I)}$ , we have following error estimates for the given method:

$$\|e_m\|^2 + 2\|e_{m-1}\|^2 + \frac{1}{2} \sum_{n=1}^{m-1} \|2\tilde{e}_{n+1} - e_n\|^2 \leq Ck^3, \quad \forall 2 \leq m \leq \frac{T}{k}$$

where  $C$  is a constant that depends on the parameters  $C_I, r, \sigma, \lambda$  and  $T$ .

**Proof** Consider the Eq. (5.2.1),

$$\frac{3\tilde{e}_{n+1} - 4e_n + e_{n-1}}{2k} = \mathcal{D}\tilde{e}_{n+1} + \mathcal{I}(\mathcal{E}e_n) + g_n + R_{n+1}. \tag{5.2.3}$$

Taking the inner product from both sides of the Eq. (5.2.3) with  $4k\tilde{e}_{n+1}$  and using the identity (I1) and (I4), we have

$$\begin{aligned} \|\tilde{e}_{n+1}\|^2 - \|e_n\|^2 + \|2\tilde{e}_{n+1} - e_n\|^2 - \|2e_n - e_{n-1}\|^2 + \|\tilde{e}_{n+1} - 2e_n + e_{n-1}\|^2 \\ \leq 4k\alpha\|\tilde{e}_{n+1}\|^2 + 4k\lambda C_I\|\mathcal{E}e_n\|\|\tilde{e}_{n+1}\| + 4k(g_n, \tilde{e}_{n+1}) + 4k(R_{n+1}, \tilde{e}_{n+1}). \end{aligned} \tag{5.2.4}$$

From the Eq. (5.2.2)

$$e_{n+1} - \frac{2}{3}kh_{n+1} = \tilde{e}_{n+1} - \frac{2}{3}kg_n. \tag{5.2.5}$$

Taking the inner product of (5.2.5) from both sides with itself and multiplying by three, we obtain

$$3\|e_{n+1}\|^2 + \frac{4}{3}k^2\|h_{n+1}\|^2 - 4k(e_{n+1}, h_{n+1}) = 3\|\tilde{e}_{n+1}\|^2 + \frac{4}{3}k^2\|g_n\|^2 - 4k(\tilde{e}_{n+1}, g_n). \tag{5.2.6}$$

Adding up the Eqs. (5.2.4) and (5.2.6), and noting  $(e_{n+1}, h_{n+1}) \leq 0$  and  $\|\tilde{e}_{n+1} - 2e_n + e_{n-1}\|^2 \geq 0$ , along with some calculations using some inequalities from Sect. 4.1, we get

$$\begin{aligned} \|e_{n+1}\|^2 - \|e_n\|^2 + \|\tilde{e}_{n+1}\|^2 + \frac{4}{3}k^2(\|h_{n+1}\|^2 - \|g_n\|^2) + 2[\|e_n\|^2 - \|e_{n-1}\|^2] \\ \leq 13\|e_n\|^2 + (4\alpha + \lambda C_I + 1)k\|\tilde{e}_{n+1}\|^2 + 32k\lambda C_I\|e_n\|^2 + 8k\lambda C_I\|e_{n-1}\|^2 + 4k\|R_{n+1}\|^2. \end{aligned}$$

Assuming that  $k < \frac{1}{2(4\alpha+\lambda C_I)}$ , with some basic calculations, further we obtain

$$\begin{aligned} \|e_{n+1}\|^2 - \|e_n\|^2 + \frac{1}{2}\|\tilde{e}_{n+1}\|^2 + \frac{4}{3}k^2(\|h_{n+1}\|^2 - \|g_n\|^2) + 2[\|e_n\|^2 - \|e_{n-1}\|^2] \\ \leq 13\|e_n\|^2 + 32k\lambda C_I\|e_n\|^2 + 8k\lambda C_I\|e_{n-1}\|^2 + 4k\|R_{n+1}\|^2. \end{aligned} \tag{5.2.7}$$

Summing up both sides of the Eq. (5.2.7) from  $n = 1$  to  $m - 1$  and perform some mathematical calculations, we get

$$\begin{aligned} & \|e_m\|^2 + 2\|e_{m-1}\|^2 + \frac{1}{2} \sum_{n=1}^{m-1} \|\tilde{e}_{n+1}\|^2 + \frac{4}{3}k^2\|h_m\|^2 \\ & \leq \|e_1\|^2 + 2\|e_0\|^2 + \frac{4}{3}k^2\|h_1\|^2 + (40k\lambda\mathcal{C}_I + 13) \sum_{n=0}^{m-1} \|e_n\|^2 + 4k \sum_{n=1}^{m-1} \|R_{n+1}\|^2 \\ & \quad + \frac{4}{3}k^2 \sum_{n=1}^{m-1} (ck^2 + ck\|h_n\|^2). \end{aligned}$$

Applying Lemma 1, we get

$$\begin{aligned} & \|e_m\|^2 + 2\|e_{m-1}\|^2 + \frac{1}{2} \sum_{n=1}^{m-1} \|\tilde{e}_{n+1}\|^2 + \frac{4}{3}k^2\|h_m\|^2 \\ & \leq C \left( \|e_1\|^2 + 2\|e_0\|^2 + \frac{4}{3}k^2\|h_1\|^2 + 4k \sum_{n=1}^{m-1} \|R_{n+1}\|^2 + \frac{4}{3}k^2 \sum_{n=1}^{m-1} (ck^2 + ck\|h_n\|^2) \right). \end{aligned}$$

Further simplifying the equation, we get the desired result

$$\|e_m\|^2 + 2\|e_{m-1}\|^2 + \frac{1}{2} \sum_{n=1}^{m-1} \|\tilde{e}_{n+1}\|^2 \leq Ck^3.$$

□

It is important to keep in mind that the limitations on  $k$  in the aforementioned theorems are only adequate for stability. These limitations can be marginally altered with more accurate analysis.

## 6 Numerical discussion

In this section, we provided some numerical examples to reinforce our theoretical study. In order to determine the price of the American option under Kou’s and Merton’s jump-diffusion models, we explored the convergence behavior of both the IMEX-BDF1-OS and IMEX-BDF2-OS numerical techniques. To tackle the inequality constraints in the LCP for the American option, we used the implicit–explicit backward difference approaches in conjunction with the operator splitting method. For spatial discretization, we employ the second-order central finite difference schemes

$$\begin{aligned} u_x(x_i) & \approx \frac{u_{i+1} - u_{i-1}}{2h}, \\ u_{xx}(x_i) & \approx \frac{u_{i+1} - 2u_i + u_{i-1}}{h^2}, \end{aligned}$$

with uniform spatial mesh length  $h$  in the computational domain  $\Omega := [-1.5, 1.5]$ .

Since for the American option pricing problem, the analytical form of solution is not available so we computed the point-wise errors at different asset prices,  $S = 90, 100, 110$ , using the difference between successive option prices.



**Table 1** Numerical results of IMEX-BDF1-OS method under Merton’s jump-diffusion model for American put options with specified parameters at various stock prices as given in Example

N	S = 90			S = 100			S = 110		
	Value	Error	Rate	Value	Error	Rate	Value	Error	Rate
64	10.454172	–	–	4.901017	–	–	2.878383	–	–
128	10.454664	4.92e–04	–	4.906693	5.68e–03	–	2.881250	2.87e–03	–
256	10.455038	3.74e–04	0.40	4.909613	2.92e–03	0.96	2.882723	1.47e–03	0.96
512	10.455287	2.48e–04	0.60	4.911114	1.50e–03	0.96	2.883477	7.54e–04	0.97
1024	10.455451	1.64e–04	0.60	4.911884	7.71e–04	0.96	2.883861	3.84e–04	0.97

**Table 2** Numerical results of IMEX-BDF2-OS method under Merton’s jump-diffusion model for American put options with specified parameters at various stock prices as given in Example 1

N	S = 90			S = 100			S = 110		
	Value	Error	Rate	Value	Error	Rate	Value	Error	Rate
64	10.456521	–	–	4.911746	–	–	2.883627	–	–
128	10.456092	4.29e–04	–	4.912395	6.49e–04	–	2.884030	4.03e–04	–
256	10.455851	2.41e–04	0.84	4.912602	2.07e–04	1.64	2.884177	1.47e–04	1.46
512	10.455737	1.15e–04	1.06	4.912666	6.39e–05	1.69	2.884230	5.37e–05	1.45
1024	10.455696	4.07e–05	1.49	4.912685	1.90e–05	1.74	2.884249	1.84e–05	1.54

To determine the rate of convergence (Rate) of given methods at different asset prices, we used the double mesh principle. The rate of convergence can be computed by the formula,

$$\text{Rate} = \log_2 \frac{\|u(k, h) - u(\frac{k}{2}, \frac{h}{2})\|}{\|u(\frac{k}{2}, \frac{h}{2}) - u(\frac{k}{4}, \frac{h}{4})\|},$$

where  $u(k, h)$  is the computed price of the American put option with temporal mesh length  $k$  and spatial mesh length  $h$ .

We used the piecewise cubic Hermite interpolation to analyze the pricing of the American put option at the non-mesh points of stock prices.

Throughout all of the tests, we calculated the point-wise errors at different stock prices  $S$  with  $M = 2^{10} + 1$  spatial discretization points, and  $N$  denotes temporal discretization points. To perform numerical simulation, the following set of examples are taken:

**Example 1** The Merton’s jump-diffusion model for the American put option along with the parameters  $\sigma = 0.15, r = 0.04, T = 0.5, K = 100, \sigma_J = 0.45, \mu_J = -0.90, \lambda = 0.10$ .

In the first numerical simulation, we showed the numerical results for the IMEX-BDF1-OS method under Merton’s model, and the option values along with point-wise errors and Rates at different asset prices are reported in Table 1. We can observe that the convergence rate reached its asymptotic order when the temporal mesh is sufficiently small.

In the same lineup, we executed the same numerical simulation for the IMEX-BDF2-OS method for Merton’s model, and the results are reported in Table 2. We see that IMEX-BDF1-OS is linearly convergent, and the rate of convergence for the IMEX-BDF2-OS method is near 1.5, which is similar to our error estimate showed in Sect. 5.

The American put option values for IMEX-BDF1-OS and IMEX-BDF2-OS under Merton’s jump-diffusion model are presented in Fig. 1, and the graphs demonstrate that the option

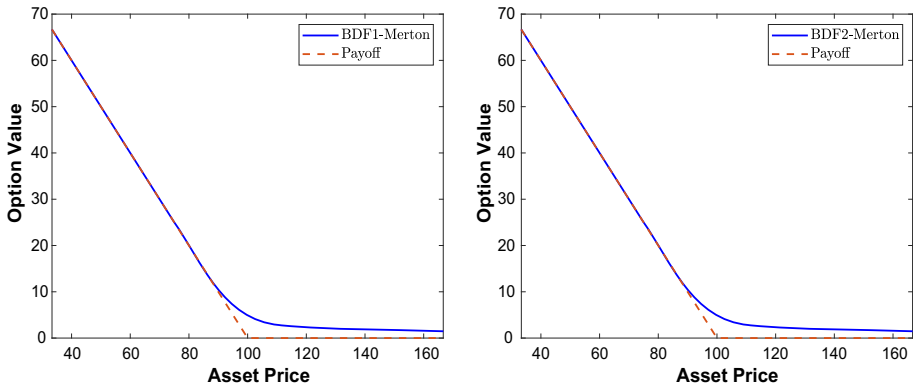


**Fig. 1** American put option value for IMEX-BDF1-OS (left) and IMEX-BDF2-OS (right) under the Merton’s jump-diffusion model with parameters as provided in the Example 1

**Table 3** Numerical results of IMEX-BDF1-OS method under Kou’s jump-diffusion model for American put options with specified parameters at various stock prices as given in Example 2

N	S = 90			S = 100			S = 110		
	Value	Error	Rate	Value	Error	Rate	Value	Error	Rate
64	10.332776	–	–	4.008922	–	–	1.353754	–	–
128	10.333855	1.08e–03	–	4.014711	5.79e–03	–	1.355915	2.16e–03	–
256	10.334494	6.39e–04	0.76	4.017678	2.97e–03	0.96	1.357037	1.12e–03	0.95
512	10.334865	3.71e–04	0.79	4.019205	1.53e–03	0.96	1.357620	5.83e–04	0.94
1024	10.335081	2.16e–04	0.78	4.019989	7.84e–04	0.96	1.357921	3.01e–04	0.95

values are quite stable with no erroneous oscillation at or near the strike price.

**Example 2** The Kou’s jump-diffusion model for American put option along with the parameters  $\sigma = 0.15$ ,  $r = 0.04$ ,  $T = 0.5$ ,  $K = 100$ ,  $\eta_1 = 3.0465$ ,  $\eta_2 = 3.0775$ ,  $p = 0.3445$ ,  $\lambda = 0.10$ .

Now, we executed similar simulation for IMEX-BDF1-OS and IMEX-BDF2-OS method for Kou’s model, and numerical results are reported in Tables 3 and 4, respectively, and we can see that IMEX-BDF1-OS is linearly convergent and for IMEX-BDF2-OS method the error is reducing with ratio nearly three thus the discretization scheme is convergent with rate 1.5, as shown in Table 4 that is similar to our error estimate.

The option values for IMEX-BDF1-OS and IMEX-BDF2-OS under Kou’s jump-diffusion model for American put options are presented in Fig. 2, and the graphs demonstrate that the option values are quite stable with no erroneous oscillation at or near the strike price.

From both examples, we showed that the pointwise errors have a convergence rate of 1.5 for IMEX-BDF2-OS and 1 for IMEX-BDF1-OS, although the order of convergence at the early exercise border is less precise for both Merton’s and Kou’s models.

**Table 4** Numerical results of IMEX-BDF2-OS method under Kou's jump-diffusion model for American put options with specified parameters at various stock prices as given in Example 2

N	S = 90		S = 100		S = 110	
	Value	Error	Value	Error	Value	Error
64	10.335902	-	4.019887	-	1.357578	-
128	10.335621	2.81e-04	4.020513	6.26e-04	1.357990	4.12e-04
256	10.335455	1.66e-04	4.020711	1.97e-04	1.358144	1.53e-04
512	10.335378	7.67e-05	4.020775	6.40e-05	1.358202	5.86e-05
1024	10.335354	2.48e-05	4.020798	2.35e-05	1.358225	2.30e-05

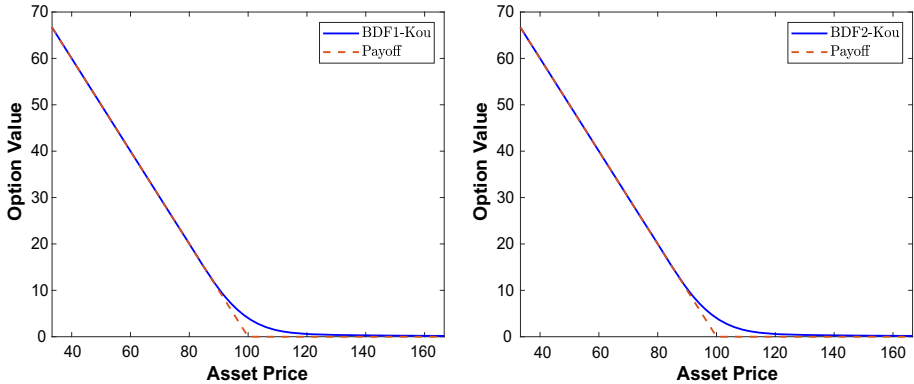


**Fig. 2** American put option value for IMEX-BDF1-OS (left) and IMEX-BDF2-OS (right) under the Kou's jump-diffusion model with parameters as provided in the Example 2

## 7 Conclusion

In this work, we established the stability and error estimates for the operator splitting method combined with implicit–explicit backward difference techniques for American option pricing problems under jump-diffusion models. The solution of the linear complementarity problem (2.0.2) is the value of the American put option under the jump-diffusion model. We have approximated the integral operator by a numerical quadrature rule. In contrast, the differential operator is computed with the help of the finite difference operator analogous to the implicit–explicit backward difference techniques. To validate our theoretical results and demonstrate the convergence behaviors of operating splitting methods, we performed the numerical computations for the American put option under both Kou's and Merton's jump-diffusion models and presented the plots for the values of American put options. In our future work, we are interested in refining the rigorous error analysis of the IMEX-BDF2-OS method up to the second order using the variable step-size IMEX-BDF approach as suggested in Wang et al. (2019) and explore the rigorous analysis for other classes of problems.

**Acknowledgements** We would like to show our gratitude to the Dr. Lok Pati Tripathi, Department of Mathematics, Indian Institute of Technology Goa, India for sharing his valuable thoughts with us throughout this research. The work of author [Deepak Kumar Yadav] is supported by the University Grants Commission(UGC), India (Student ID-DEC18-416341).

**Data availability** Not Applicable.

## Declarations

**Conflict of interest** The authors declare that they have no conflict of interest.

## References

- Akbari R, Mokhtari R, Jahandideh MT (2019) A combined compact difference scheme for option pricing in the exponential jump-diffusion models. *Adv Differ Equ* 1:1–3
- Bastani AF, Ahmadi Z, Damircheli D (2013) A radial basis collocation method for pricing American options under regime-switching jump-diffusion models. *Appl Numer Math* 65:79–90

- Boen L, In't Hout KJ (2020) Operator splitting schemes for American options under the two-asset Merton jump-diffusion model. *Appl Numer Math* 153:114–31
- Chen F, Shen J (2020) Stability and error analysis of operator splitting methods for American options under the Black–Scholes model. *J Sci Comput* 82(2):1–17
- Chen F, Shen J, Haijun Y (2012) A new spectral element method for pricing European options under the Black–Scholes and Merton jump diffusion models. *J Sci Comput* 52(3):499–518
- Chen C, Wang Z, Yang Y (2019) A new operator splitting method for American options under fractional Black–Scholes models. *Comput Math Appl* 77(8):2130–2144
- Chen Y, Xiao A, Wang W (2019) An IMEX-BDF2 compact scheme for pricing options under regime-switching jump-diffusion models. *Math Methods Appl Sci* 42(8):2646–2663
- Cho J, Kim Y, Lee S (2022) An accurate and stable numerical method for option hedge parameters. *Appl Math Comput* 430:127276
- Company R, Egorova VN, Jódar L (2021) A front-fixing ETD numerical method for solving jump-diffusion American option pricing problems. *Math Comput Simul* 189:69–84
- Cont R, Voltchkova E (2005) A finite difference scheme for option pricing in jump diffusion and exponential Lévy models. *SIAM J Numer Anal* 43(4):1596–1626
- Dehghan M, Bastani AF et al (2018) On a new family of radial basis functions: mathematical analysis and applications to option pricing. *J Comput Appl Math* 328:75–100
- del Carmen Calvo-Garrido M, Vázquez C (2015) Effects of jump-diffusion models for the house price dynamics in the pricing of fixed-rate mortgages, insurance and coinsurance. *Appl Math Comput* 271:730–742
- Düring B, Pitkin A (2019) High-order compact finite difference scheme for option pricing in stochastic volatility jump models. *J Comput Appl Math* 355:201–217
- Garroni MG, Menaldi JL et al (1992) Green functions for second order parabolic integro-differential problems, vol 275. Chapman and Hall/CRC
- Haghi M, Mollapourasl R, Vanmaele M (2018) An RBF-FD method for pricing American options under jump-diffusion models. *Comput Math Appl* 76(10):2434–2459
- Huang Y, Forsyth PA, Labahn G (2011) Methods for pricing American options under regime switching. *SIAM J Sci Comput* 33(5):2144–2168
- Huang J, Cen Z, Le A (2013) A finite difference scheme for pricing American put options under Kou's jump-diffusion model. *J Funct Spaces Appl*
- Ikonen S, Toivanen J (2004) Operator splitting methods for American option pricing. *Appl Math Lett* 17(7):809–814
- Ikonen S, Toivanen J (2009) Operator splitting methods for pricing American options under stochastic volatility. *Numer Math* 113(2):299–324
- Kadalbajoo MK, Kumar A, Tripathi LP (2015) Application of the local radial basis function-based finite difference method for pricing American options. *Int J Comput Math* 92(8):1608–1624
- Kadalbajoo MK, Tripathi LP, Kumar A (2015) Second order accurate IMEX methods for option pricing under Merton and Kou jump-diffusion models. *J Sci Comput* 65(3):979–1024
- Kadalbajoo MK, Kumar A, Tripathi LP (2016) A radial basis function based implicit-explicit method for option pricing under jump-diffusion models. *Appl Numer Math* 110:159–173
- Kazmi K (2019) An IMEX predictor-corrector method for pricing options under regime-switching jump-diffusion models. *Int J Comput Math* 96(6):1137–1157
- Kou SG (2002) A jump-diffusion model for option pricing. *Manage Sci* 48(8):1086–1101
- Kumar D, Deswal K (2021) Haar-wavelet based approximation for pricing American options under linear complementarity formulations. *Numer Methods Partial Differ Equ* 37(2):1091–1111
- Kwon Y, Lee Y (2011) A second-order tridiagonal method for American options under jump-diffusion models. *SIAM J Sci Comput* 33(4):1860–1872
- Li H, Mollapourasl R, Haghi M (2019) A local radial basis function method for pricing options under the regime switching model. *J Sci Comput* 79(1):517–541
- Matache A-M, Von Petersdorff T, Schwab C (2004) Fast deterministic pricing of options on Lévy driven assets. *ESAIM Math Model Numer Anal* 38(1):37–71
- Merton RC (1976) Option pricing when underlying stock returns are discontinuous. *J Financ Econ* 3(1–2):125–144
- Mollapourasl R, Haghi M, Liu R (2018) Localized kernel-based approximation for pricing financial options under regime switching jump diffusion model. *Appl Numer Math* 134:81–104
- Patel KS, Mehra M (2017) Fourth-order compact finite difference scheme for American option pricing under regime-switching jump-diffusion models. *Int J Appl Comput Math* 3(1):547–567
- Patel KS, Mehra M (2018) Fourth-order compact scheme for option pricing under the Merton's and Kou's jump-diffusion models. *Int J Theor Appl Finance* 21(04):1850027

- Pindza E, Patidar KC, Ngounda E (2014) Robust spectral method for numerical valuation of European options under Merton's jump-diffusion model. *Numer Methods Partial Differ Equ* 30(4):1169–1188
- Quarteroni A, Valli A (2008) Numerical approximation of partial differential equations, vol 23. Springer, Berlin
- Rad JA, Parand K (2017) Numerical pricing of American options under two stochastic factor models with jumps using a meshless local Petrov-Galerkin method. *Appl Numer Math* 115:252–274
- Saib AAE-F, Tangman DY, Bhuruth M (2012) A new radial basis functions method for pricing American options under Merton's jump-diffusion model. *Int J Comput Math* 89(9):1164–1185
- Salmi S, Toivanen J (2011) An iterative method for pricing American options under jump-diffusion models. *Appl Numer Math* 61(7):821–831
- Salmi S, Toivanen J (2014) IMEX schemes for pricing options under jump-diffusion models. *Appl Numer Math* 84:33–45
- Shirzadi M, Dehghan M, Bastani AF (2020) On the pricing of multi-asset options under jump-diffusion processes using meshfree moving least-squares approximation. *Commun Nonlinear Sci Numer Simul* 84:105160
- Thakoor N, Tangman DY, Bhuruth M (2013) A new fourth-order numerical scheme for option pricing under the CEV model. *Appl Math Lett* 26(1):160–164
- Thakoor N, Tangman DY, Bhuruth M (2018) RBF-FD schemes for option valuation under models with price-dependent and stochastic volatility. *Eng Anal Boundary Elem* 92:207–217
- Tour G, Thakoor N, Ma J, Tangman DY (2020) A spectral element method for option pricing under regime-switching with jumps. *J Sci Comput* 83(3):1–31
- Wang W, Chen Y, Fang H (2019) On the variable two-step IMEX BDF method for parabolic integro-differential equations with nonsmooth initial data arising in finance. *SIAM J Numer Anal* 57(3):1289–1317
- Wang W, Mao M, Wang Z (2021) An efficient variable step-size method for options pricing under jump-diffusion models with nonsmooth payoff function. *ESAIM Math Model Numer Anal* 55(3):913–938
- Xu C, Su B, Liu C (2022) A quick operator splitting method for option pricing. *J Comput Appl Math* 406:113949
- Yousuf Muhammad, Khaliq AQM, Alrabeei Salah (2018) Solving complex PIDE systems for pricing American option under multi-state regime switching jump-diffusion model. *Comput Math Appl* 75(8):2989–3001

**Publisher's Note** Springer Nature remains neutral with regard to jurisdictional claims in published maps and institutional affiliations.

Springer Nature or its licensor (e.g. a society or other partner) holds exclusive rights to this article under a publishing agreement with the author(s) or other rightsholder(s); author self-archiving of the accepted manuscript version of this article is solely governed by the terms of such publishing agreement and applicable law.